

See discussions, stats, and author profiles for this publication at: <https://www.researchgate.net/publication/51660296>

# CO<sub>2</sub> Capture at Low Temperatures (30–80 °C) and in the Presence of Water Vapor over a Thermally Activated Mg–Al Layered Double Hydroxide

ARTICLE *in* THE JOURNAL OF PHYSICAL CHEMISTRY A · SEPTEMBER 2011

Impact Factor: 2.69 · DOI: 10.1021/jp207836m · Source: PubMed

---

CITATIONS

8

---

READS

73

## 4 AUTHORS, INCLUDING:



**Enrique Lima**

Universidad Nacional Autónoma de México

103 PUBLICATIONS 1,038 CITATIONS

SEE PROFILE



**Jaime S Valente**

Instituto Mexicano del Petroleo

96 PUBLICATIONS 1,587 CITATIONS

SEE PROFILE



**Heriberto Pfeiffer**

Universidad Nacional Autónoma de México

108 PUBLICATIONS 1,471 CITATIONS

SEE PROFILE

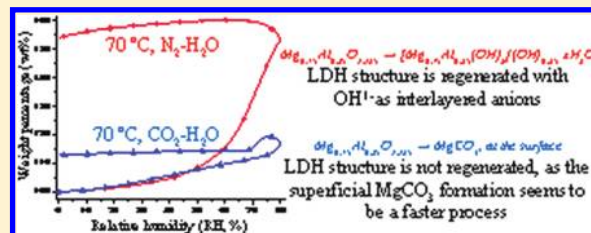
# CO<sub>2</sub> Capture at Low Temperatures (30–80 °C) and in the Presence of Water Vapor over a Thermally Activated Mg–Al Layered Double Hydroxide

Daniela A. Torres-Rodríguez,<sup>†</sup> Enrique Lima,<sup>†</sup> Jaime S. Valente,<sup>‡</sup> and Heriberto Pfeiffer<sup>\*,†</sup>

<sup>†</sup>Instituto de Investigaciones en Materiales, Universidad Nacional Autónoma de México, Circuito exterior s/n, Cd. Universitaria, Del. Coyoacán, CP 04510, México DF, Mexico

<sup>‡</sup>Instituto Mexicano del Petróleo, Eje Central 152, CP 07730, México DF, Mexico

**ABSTRACT:** The carbonation process of a calcined Mg–Al layered double hydroxide (LDH) was systematically analyzed at low temperatures, varying the relative humidity. Qualitative and quantitative experiments were performed. In a first set of experiments, the relative humidity was varied while maintaining a constant temperature. Characterization of the rehydrated products by thermogravimetric analysis (TGA), Fourier transform infrared spectroscopy (FTIR) and solid-state NMR revealed that the samples did not recover the LDH structure; instead hydrated MgCO<sub>3</sub> was produced. The results were compared with similar experiments performed on magnesium oxide for comparison purposes. Then, in the second set of experiments, a kinetic analysis was performed. The results showed that the highest CO<sub>2</sub> capture was obtained at 50 °C and 70% of relative humidity, with a CO<sub>2</sub> absorption capacity of 2.13 mmol/g.



## INTRODUCTION

Fossil fuel burning power plants constitute the greatest anthropogenic source of carbon dioxide (CO<sub>2</sub>) emissions. Therefore, in past years, a special emphasis has been set on studying the separation of CO<sub>2</sub> from flue gases of fixed sources.<sup>1–3</sup> In that sense, different kinds of materials have been studied as possible CO<sub>2</sub> captors, such as organic sorbents,<sup>4–6</sup> zeolites,<sup>7–10</sup> activated carbons,<sup>11–14</sup> alkaline ceramics,<sup>15–18</sup> calcium and magnesium oxides,<sup>19–23</sup> and hydrotalcites.<sup>1,24–27</sup>

Among these materials, the family of layered double hydroxides (LDHs), also known as hydrotalcite-like compounds, comprises interesting kinds of materials. LDHs have been used in different applications, such as PVC additives, flame retardants, hybrid composites, anion-exchangers and catalysts.<sup>28–36</sup> The basic structure of an LDH resembles that of brucite, Mg(OH)<sub>2</sub>, wherein partial isomorphous substitution of M<sup>2+</sup> by M<sup>3+</sup> cations renders positively charge layers. This charge is balanced by anions located in the interlayer region along with hydration water molecules. Given the variety of isostructural materials that may be prepared, LDHs are represented by the general formula [M<sup>2+</sup><sub>(1-x)</sub>M<sup>3+</sup><sub>x</sub>(OH)<sub>2</sub>] A<sup>n-</sup><sub>x/n</sub> · mH<sub>2</sub>O. The divalent and trivalent cations may be any such cations whose ionic radii are close to that of Mg<sup>2+</sup>, while A<sup>n-</sup> may be virtually any organic or inorganic anion.

Many interesting properties of LDHs derive from their remarkable thermal behavior, as calcination of an LDH at 400–700 °C yields a mixed metal oxide solid solution. These mixed oxides present relatively large specific surface areas and an excellent dispersion of the metal components, making them

attractive for numerous applications. Furthermore, the calcined LDHs may recover the original layered structure when contacted with an anion in aqueous solution, or simply by ambient moisture; this property is known as the memory effect.<sup>28–30,37</sup>

In past years, different reports have been published regarding the use of LDHs as CO<sub>2</sub> sorbents.<sup>1,24,27,38–48</sup> In general, LDHs do not present the best CO<sub>2</sub> capture capacities, compared to other materials used in this field. In order to improve the CO<sub>2</sub> sorption capacity of LDH materials, different alternatives have been proposed: for instance, the addition of alkaline metals (e.g., potassium) to increase basicity,<sup>27,38</sup> modification of M<sup>2+</sup> and M<sup>3+</sup> structural metals,<sup>39,44</sup> or a pressure increase.<sup>45,46,48</sup> Also, CO<sub>2</sub> capture has been attempted at relatively high temperatures (300–600 °C), at which the original layered structure is collapsed and the Mg(Al)O periclase-like mixed oxide is produced. In this case, CO<sub>2</sub> is trapped either by physisorption or by chemisorption, forming carbonates and/or bicarbonates.

Water steam is a common component of flue gases emitted from different combustion processes. Therefore, it is very important to analyze how CO<sub>2</sub> capture is modified due to the presence of water vapor on the different sorbents. The effect of water as vapor or liquid during CO<sub>2</sub> capture on thermally calcined LDH structures has been studied, and there is a general agreement in the fact that water seems to enhance the CO<sub>2</sub> capture on these materials. In those cases where CO<sub>2</sub> is chemisorbed, the improvements observed due to water addition have

Received: August 15, 2011

Published: September 21, 2011

been explained by a sequential reaction mechanism, in which MgO reacts initially with water, producing  $\text{Mg}(\text{OH})_2$ . Then, as  $\text{Mg}(\text{OH})_2$  seems to be more reactive to  $\text{CO}_2$  than MgO, the  $\text{CO}_2$  capture is increased, obtaining  $\text{MgCO}_3$  as the final product.<sup>41</sup> All these works have been performed at  $T \geq 200^\circ\text{C}$  and, in several cases, using potassium or sodium as additives.<sup>1,27,41,49</sup>

On the other hand, if water adsorption were carried out at low temperatures, the thermally treated LDH sample might recover its layered structure.<sup>37,50</sup> Therefore, the aim of the present work was to study the  $\text{CO}_2$  capture on a calcined  $\text{Mg}(\text{Al})\text{O}$  mixed oxide, derived from an LDH with a Mg/Al molar ratio equal to 3. The process was carried out at low temperatures ( $30\text{--}80^\circ\text{C}$ ) and varying the relative humidity (RH), in order to analyze whether the carbonation process occurs in a similar way to that observed at high temperatures, or if the layered structure is recovered, due to the presence of water vapor, incorporating carbonates ( $\text{CO}_3^{2-}$ ) as charge-balancing anions.

## EXPERIMENTAL SECTION

Mg–Al LDH, with a Mg/Al molar ratio of 3, was prepared by coprecipitation at low supersaturation, according to previously reported methods,<sup>37</sup> using hexahydrated magnesium nitrate ( $\text{Mg}(\text{NO}_3)_2 \cdot 6\text{H}_2\text{O}$ , Aldrich) and nonahydrated aluminum nitrate ( $\text{Al}(\text{NO}_3)_3 \cdot 9\text{H}_2\text{O}$ , Aldrich). The original sample was labeled as native LDH. Then, a portion of this sample was heat-treated at  $550^\circ\text{C}$  for 4 h, prior to  $\text{CO}_2$  capture tests; this sample was labeled as calcined LDH.

Native and calcined LDH samples were characterized by X-ray diffraction (XRD) and  $\text{N}_2$  adsorption. The XRD patterns were obtained using a diffractometer D8 Advance-Bruker coupled to a copper anode X-ray tube. The presence of pure LDH (native sample) and periclase (sample thermally activated) structures were confirmed by fitting the diffraction patterns with the corresponding Joint Committee Powder Diffraction Standards (JCPDS). Additionally, the nitrogen adsorption–desorption isotherms and surface area analyses were determined with Bel-Japan Minisorp II equipment, using a multipoint technique. Samples were previously degasified at room temperature for 24 h in vacuum.

$\text{CO}_2$  sorption experiments were performed in a water vapor environment between  $30$  and  $80^\circ\text{C}$ . Dynamic  $\text{CO}_2$ –water vapor sorption experiments were carried out on a temperature-controlled thermobalance TA Instruments model Q5000SA, equipped with a humidity-controlled chamber, varying temperature, time, and RH. All the experiments were carried out using  $\text{CO}_2$  (Praxair, grade 3.0) as carrier gas, distilled water, and around  $3\text{--}5$  mg of calcined LDH. The  $\text{CO}_2$  flow used was  $100\text{ mL/min}$ , and the RH percentages were controlled automatically with the Q5000SA equipment. First, water vapor sorption/desorption isotherms were generated at temperatures between  $40$  and  $80^\circ\text{C}$ , varying the RH from  $0$  to  $80\%$  and back, at a rate of  $0.5\text{ RH\% per minute}$ , using an autosampler, which may induce further adsorption processes. Additionally, different adsorption curves were obtained maintaining a constant RH ( $30, 40, 50, 60$  and  $70\%$ ), but increasing temperature from  $40$  to  $70^\circ\text{C}$ . Furthermore, the isothermal experiments were performed at different temperatures ( $40, 50, 60$ , and  $70^\circ\text{C}$ ) and RH ( $40, 50, 60$  and  $70\%$ ). For the isothermal experiments, each sample was immediately analyzed by thermogravimetric analysis (TGA) or Fourier transform infrared spectroscopy (FTIR) after the experiment, in order to eliminate further environmental sorption processes. It has to be

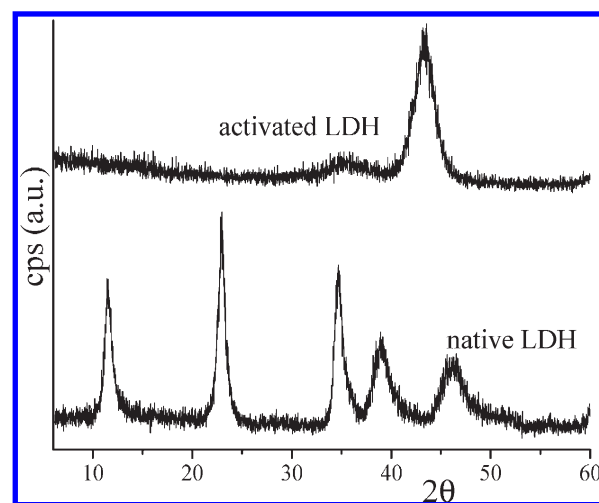


**Figure 1.** XRD patterns of the native and thermally activated ( $550^\circ\text{C}$ ) LDH samples.

mentioned that results were corroborated repeating several of the experiments with different sets of samples.

After the  $\text{CO}_2$ –water sorption experiments, and in order to identify the hydration products, the products were characterized by standard TGA, FTIR, XRD, and solid-state nuclear magnetic resonance spectroscopy (NMR). TG experiments were performed under air atmosphere, with a heating rate of  $5^\circ\text{C/min}$  in a thermobalance TA Instruments model Q500HR. For the FTIR spectroscopy, samples were analyzed on a Spectrometer NICOLET 6700 FT-IR. XRD was performed in a diffractometer (Bruker AXS, D8 Advance) coupled to a copper anode X-ray tube. Compounds were identified by the corresponding Joint Committee Powder Diffraction Standards (JCPDS).  $^{27}\text{Al}$  MAS NMR spectra were acquired with a  $4\text{ mm}$  probe on an Avance II Bruker spectrometer at an operating frequency for  $^{27}\text{Al}$  of  $78.15\text{ MHz}$ . Small  $^{27}\text{Al}$  flip angles of  $\pi/12$ , pulse delays of  $0.5\text{ s}$ , and a spinning speed of  $10\text{ kHz}$  were used for the data collection. Chemical shifts are referenced to  $1\text{ M}$  solution of aluminum chloride ( $\text{AlCl}_3$ ).

## RESULTS AND DISCUSSION

Both LDH samples (native and thermally activated at  $550^\circ\text{C}$ ) were characterized by XRD. These results are present in Figure 1. Native and activated LDH samples fitted very well with the LDH  $\text{Mg}_6\text{Al}_2(\text{OH})_{18} \cdot 4\text{H}_2\text{O}$  (JCPDS 38-0478) and the MgO periclase (JCPDS file 30-0794) structures, respectively. These results confirmed the correct synthesis and thermal activation of samples. The activated LDH sample presented broad peaks, which indicate the formation of crystals with small sizes. Additionally, the textural properties of both samples were determined by  $\text{N}_2$  adsorption–desorption (data not shown). In both cases, the samples presented type IV isotherms, which are attributed to mesoporous materials. Additionally, the native and activated samples presented the following BET surface areas:  $87$  and  $216\text{ m}^2/\text{g}$ , respectively.

Different water vapor sorption/desorption isotherms were measured, at different temperatures, using  $\text{CO}_2$  as the carrier gas (Figure 2). All the calcined LDH samples presented type III isotherms.<sup>51</sup> The adsorption process is irreversible; all samples show a  $12\text{--}14\text{ wt\%}$  increment after the desorption process is done. These mass increments could be attributed to nonreversible

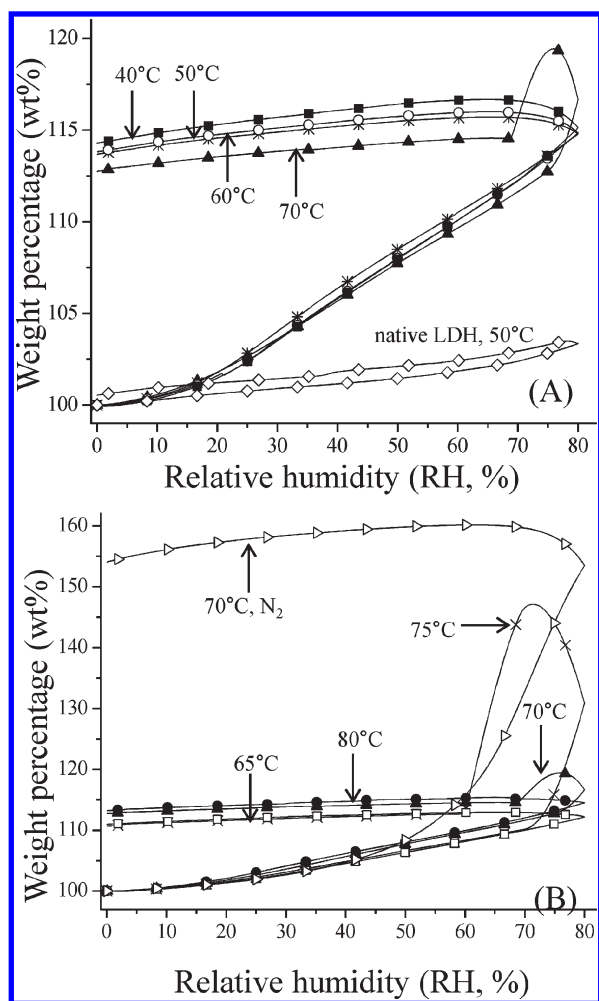


**Figure 2.** Water sorption/desorption isotherms on the calcined LDH sample, generated at different temperatures using CO<sub>2</sub> as carrier gas: (A) 40, 50, 60, and 70 °C; (B) 65, 70, 75, 80 °C. Additionally, the N<sub>2</sub> water sorption/desorption isotherm at 70 °C was included (B), as well as the native LDH sample at 50 °C with CO<sub>2</sub>, both for comparison purposes.

structural modifications due to sorbed water and/or CO<sub>2</sub> molecules. On the other hand, although the native LDH sample presented the same kind of isotherms (type III), the observed weight increment of ~3 wt % is small compared with the calcined LDH sample. This behavior suggests that CO<sub>2</sub>–water sorption/desorption processes are practically reversible on the native LDH sample (Figure 2A). The calcined LDH sample presented an atypical behavior between 70 and 75 °C (Figure 2B). In this temperature range, isotherms increased their weight very importantly when RH reached values between 60 and 80%. It may be explained as some kind of water adsorption produced over the particle surfaces. However, at temperatures equal to or higher than 80 °C, the water evaporation rate is considerably increased, hindering the water condensation.

In a previous work,<sup>37</sup> the behavior of a calcined LDH sample was studied under different temperature and RH conditions, using N<sub>2</sub> as a carrier gas instead of CO<sub>2</sub> and with the same flow, 100 mL/min. In that case, the layered structure was totally regenerated. Here, one of these experiments was reproduced; obtaining identical results (see 2B), which indicates the reproducibility.

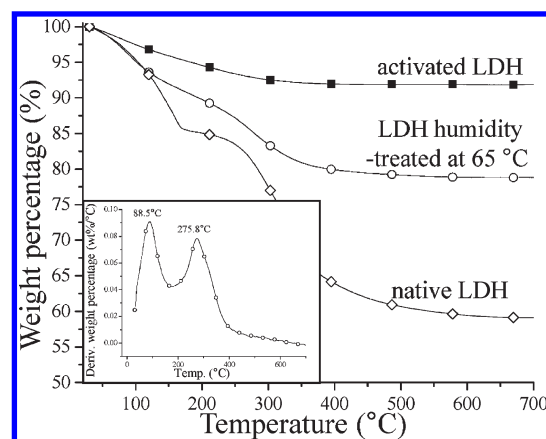
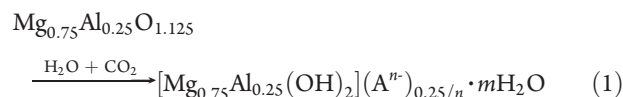


**Figure 3.** TGA curves of different LDH samples. The square inset shows the DTGA curve of the calcined LDH humidity treated at 65 °C.

The weight increment in this case is ~55 wt %. However, when CO<sub>2</sub> was used as the carrier gas, the samples only gained around 12.5–14 wt %. If periclase were to recover the original LDH structure, in the presence of H<sub>2</sub>O and CO<sub>2</sub>, the following reaction should occur (reaction 1):



where, A<sup>n−</sup> could be either OH<sup>1−</sup> or CO<sub>3</sub><sup>2−</sup>, or combinations. However, any of these possible regeneration processes would imply weight increments of at least 45–48.8 wt %. In fact, a recrystallization process, from periclase to the LDH structure, necessarily must be accompanied by intercalation of water molecules. Therefore, the presence of CO<sub>2</sub> as carrier gas or the selected gas flow (100 mL/min) during water sorption isotherms must change the kinetic behavior of the periclase–LDH regeneration, reducing the regeneration rate, varying the kinetic regime on the solid–gas interface, and/or changing the reactivity and generating different products.<sup>52,53</sup> Therefore, in order to analyze and identify the hydration products obtained during the H<sub>2</sub>O–CO<sub>2</sub> sorption isotherms, different humidity-treated samples were analyzed using TGA, FTIR, and solid-state NMR.

Figure 3 shows the TG analyses of a native and a calcined LDH, and of a humidity-treated (65 °C) LDH sample. The native LDH sample presented two well-defined weight losses: (1) Initially, it lost 14.8 wt % attributed to the dehydration processes (between room temperature and 170 °C) of superficial and interlayer water; (2) then, the sample lost 26.2 wt %, which corresponded to dehydroxylation and decarbonation processes (between 220 and 500 °C). The calcined LDH sample lost 7.5 wt % in total, which corresponded to two different processes: a dehydration (75.1 °C) and a dehydroxylation (212.3 °C). This sample must have trapped water spontaneously from the environment, which produced these two processes. On the other hand, the sample humidity-treated with CO<sub>2</sub> at 65 °C lost 3 times more weight (21.3 wt %) than the calcined LDH sample, as could be expected, due to different sorption processes occurring during the isothermal experiments. Nevertheless, this sample lost weight continuously, so that product identification becomes more difficult. So, in this case, the DTG-curve is presented in the square inset of Figure 3. As may be seen, two different processes were evidenced. The first one, at 88.5 °C, must correspond to



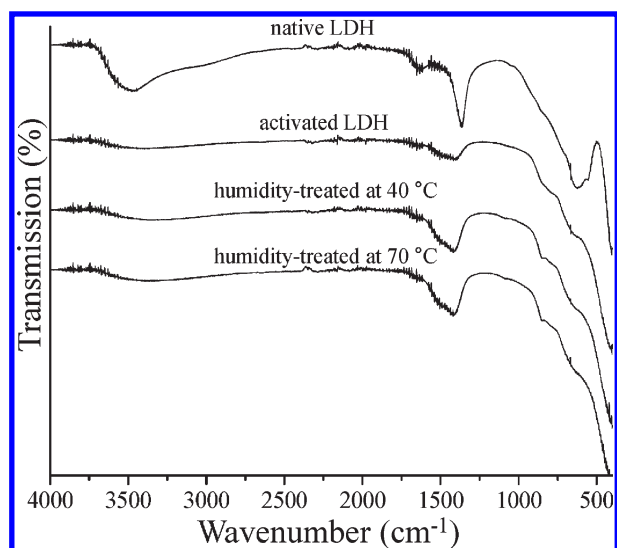


**Figure 4.** Infrared spectra of different LDH samples, before and after humidity treatments.

surface-adsorbed water, as the temperature is too low for an interlayer water loss phenomenon to be observed. This result suggests that the layered structure is not being regenerated. The second process observed for the humidity-treated sample was produced at 275.8 °C, which cannot be assigned with certainty to a specific process.

Figure 4 shows the FTIR of native and calcined LDH samples as well as different hydration products of the calcined LDH sample. The native LDH sample presented four wide vibration bands centered at 653, 1370, 1630, and 3500  $\text{cm}^{-1}$ , which correspond to Mg/Al-oxygen, carbonate, water, and hydroxyl vibrations. These bands are present in any native LDH sample containing carbonates as interlayer anions. Actually, the broad absorption band centered at 653  $\text{cm}^{-1}$  probably contains the Mg/Al–O vibration and a contribution of the band due to carbonate anion deformation, which is expected to appear close to 700  $\text{cm}^{-1}$ . After thermal treatment, the band intensity around 650–700  $\text{cm}^{-1}$  decreased significantly, in agreement with a decarbonation process and it was shifted and separated into two new vibration bands at 667 and 857  $\text{cm}^{-1}$ . Additionally, the intensity of the carbonate and hydroxyl bands diminished significantly. All these changes are in good agreement with the layered-structure destruction and the corresponding MgO periclase formation.<sup>54,55</sup> In the same figure are presented FTIR spectra of two different hydration products of the calcined LDH samples humidity-treated at 40 and 70 °C. These two spectra showed an increase of intensity of carbonate (1360  $\text{cm}^{-1}$ ) and hydroxyl (3500  $\text{cm}^{-1}$ ) absorption bands in comparison to the calcined LDH sample, with the carbonate band being the one that increased more significantly. These results indicate that the weight increments observed would be attributed to some kind of carbonation mainly, and, to minor extent, to a hydroxylation process, but different from those produced during an LDH regeneration process. Indeed, the band due to the bending vibration of water, expected close to 1630  $\text{cm}^{-1}$ , is absent, suggesting that molecular water was not formed on hydrated LDHs. Additionally, the position of the carbonate band absorption was shifted toward lower wavenumbers in the humidity-treated LDH samples if compared with the native LDH.

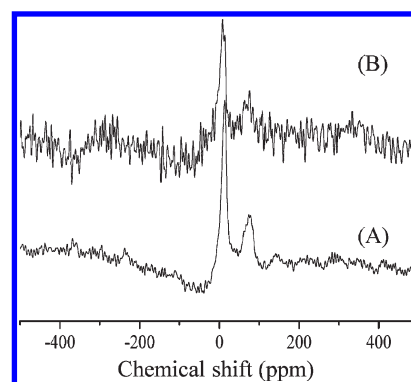


**Figure 5.**  $^{27}\text{Al}$  MAS NMR spectra of calcined (a) and humidity-treated at 70 °C (b).

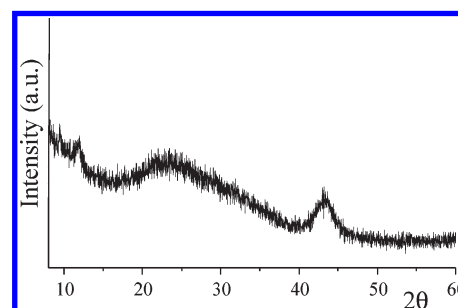


**Figure 6.** XRD pattern of the activated humidity-treated samples at 60 °C.

These results suggest that the C–O elongation could be modified as a consequence of  $\text{CO}_2$  being chemically trapped and stabilized on the calcined LDH particles surface, possibly bonded directly onto  $\text{O}^{2-}$  or  $\text{OH}^{1-}$  species. The absence of absorption bands between 2000 and 2200  $\text{cm}^{-1}$  supports the idea that  $\text{CO}_2$  does not interact weakly through hydrogen bonds, but carbonate species were formed.

$^{27}\text{Al}$  MAS NMR spectra show that the aluminum environment on the calcined LDH sample is not affected after  $\text{CO}_2$ –water adsorption–desorption isotherms (Figure 5). Both these spectra (the calcined LDH sample and the sample humidity-treated at 70 °C) presented two well-defined isotropic NMR signals. The first signal was presented close to 8 ppm, which is due to 6-fold coordinated aluminum. The second one, at 71 ppm, was assigned to 4-fold coordinated aluminum.<sup>56,57</sup> In fact, the 6-fold:4-fold intensity ratio of the coordinated aluminum signals was maintained at around 2.4 in both samples. These results confirm that the LDH regeneration process does not occur and that the recovery of the total 6-fold coordinated aluminum environment did not occur after the  $\text{CO}_2$ –water adsorption–desorption process.

As a final characterization test one of the hydrated products (the sample treated at 60 °C) was evaluated by XRD and compared with the native and activated LDH samples (see Figures 1 and 6). It has to be mentioned that the XRD pattern of the hydrated sample shows a large amorphous signal related to the glass support as the hydrated products are around only 3 mg of the sample (Figure 6). As it can be seen, at 43.3° the most evident diffraction peak appears, which corresponds to the periclase structure. The presence of periclase is in good agreement with the previous results, where no LDH regeneration was evidenced. Additionally, although the  $\text{SiO}_2$  amorphous signal appeared at  $2\theta$  values lower than 40°, it is possible to evidence

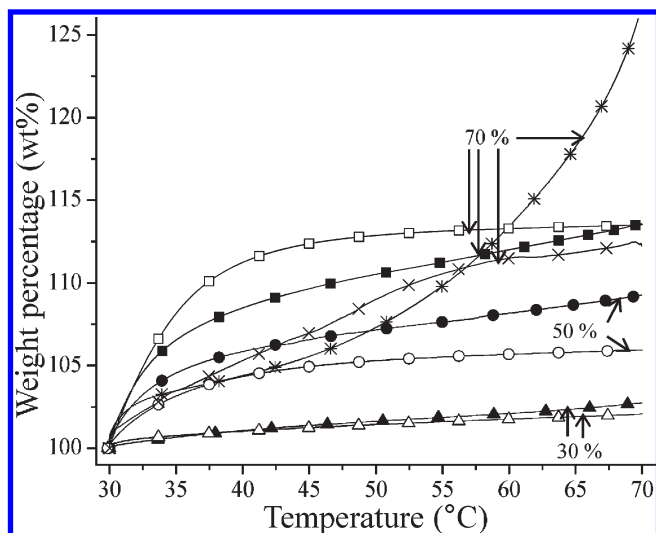


**Figure 7.** Activation temperatures of  $\text{CO}_2$  and  $\text{H}_2\text{O}$  sorption on the calcined LDH and MgO using different RHs and different carrier gases. Filled symbols: calcined LDH/ $\text{CO}_2$  carrier; empty symbols: MgO/ $\text{CO}_2$ ; \*: calcined LDH/ $\text{N}_2$ ; x: MgO/ $\text{N}_2$ .

the presence of a diffraction peak at  $11.9^\circ$ . This peak could be assigned to the 003 peak of the LDH structure. However, none of the other peaks assignable to this structure are evidenced. Additionally, the 003 peak of the native carbonated structure is located at  $11.4^\circ$ . Therefore, it does not totally fit to the LDH structure. On the other hand, this peak fits very well to a hydrated magnesium hydroxyl-carbonate ( $\text{Mg}_7(\text{CO}_3)_5(\text{OH})_4 \cdot 24\text{H}_2\text{O}$ , JCPDS file 47-1880). As a result of the different characterization techniques used for the identification of the hydrated products, it seems that the LDH structure is not recovered under these conditions of RH and  $\text{CO}_2$  as the carrier gas.

In order to compare and further understand the  $\text{CO}_2$  sorption on the calcined LDH sample, different experiments were performed on a calcined LDH, and also on MgO for comparison purposes. Different dynamic analyses were performed fixing RH at 30, 50 and 70% RH, while temperature was varied from 30 to 70 °C, using  $\text{CO}_2$  or  $\text{N}_2$  as the carrier gas (Figure 7). If  $\text{N}_2$  was used as the carrier gas at 70% RH, the LDH sample presented a weight increment divided into two different steps. Between 30 and 40 °C, the sample presented some water adsorption, then at higher temperatures water absorption began regenerating the layered structure. At this point, water reacts with the calcined LDH sample producing hydroxides, which promote the LDH

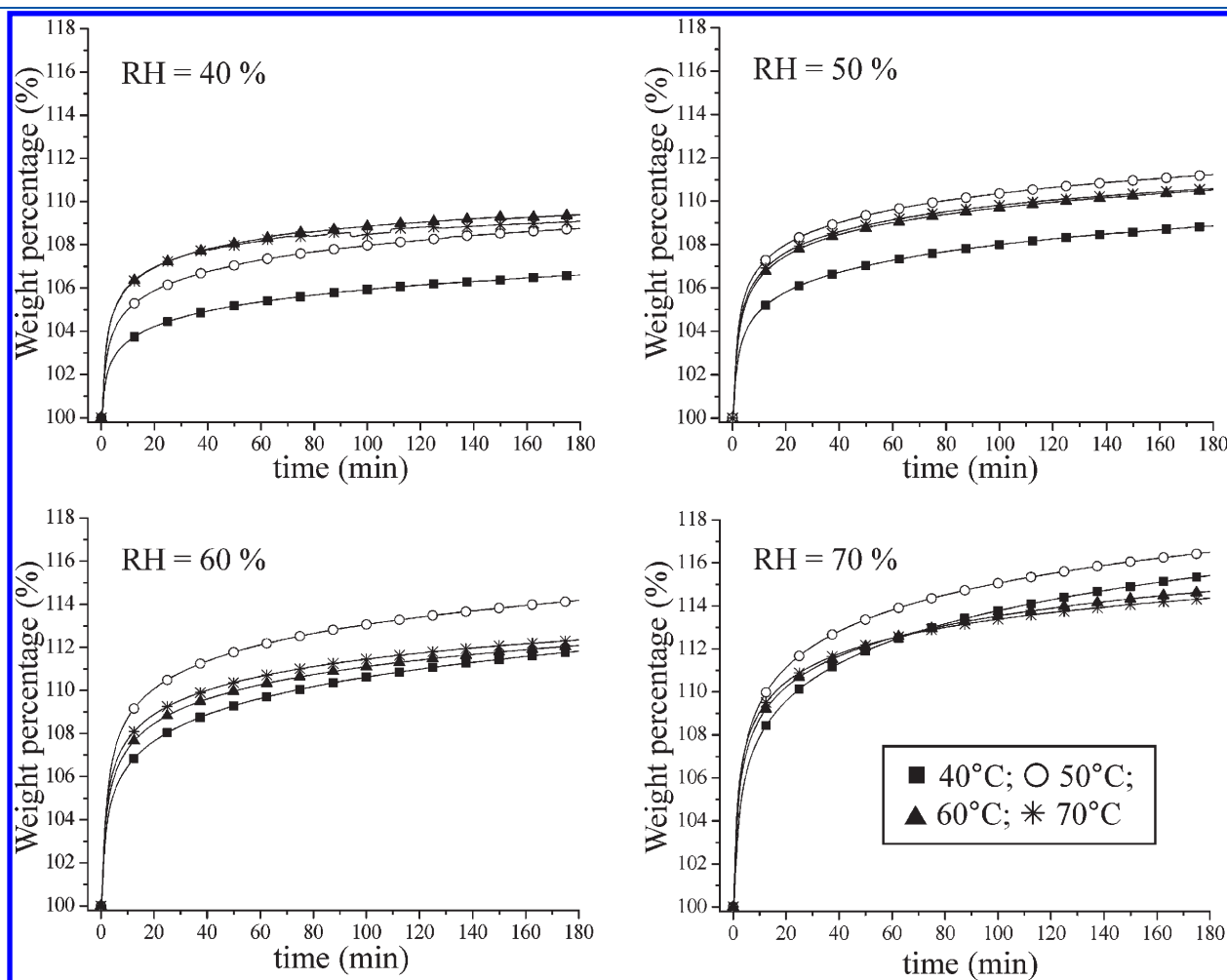


**Figure 8.** Isotherms of water sorption on the calcined LDH sample varying the temperature (from 40 to 70 °C) and RH (from 40 to 70%), using  $\text{CO}_2$  as the carrier gas.

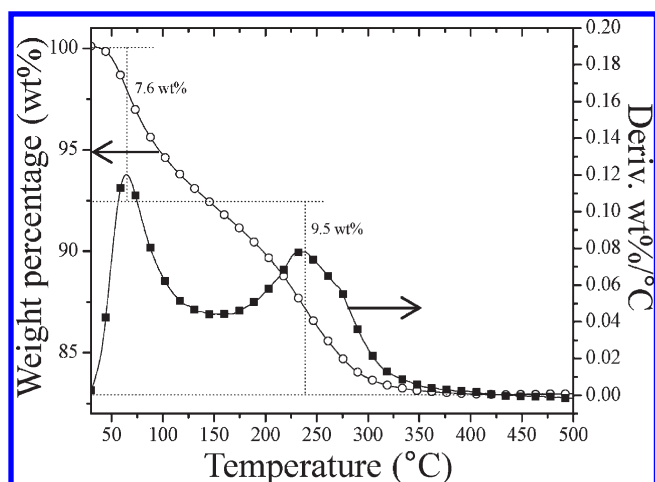


**Figure 9.** TG and DTG curves of the LDH samples humidity-treated at 50 °C with 70% RH. The thermogram was obtained at 1 °C/min.

regeneration process. This result reproduces a previous report.<sup>37</sup> In the MgO sample, the weight increment trend varied. In this case, the superficial water sorption was similar to that observed on the LDH sample. However, at higher temperatures the sorption processes were importantly reduced.

On the contrary, if CO<sub>2</sub> was used as the carrier gas, the samples presented similar dynamic experimental curves among them, but different from that observed for the LDH sample on N<sub>2</sub>. At 30 and 50% RH, both samples gained weight exponentially, and the LDH sample gained more weight than MgO, although the weight differences were higher at 50% RH. Apparently, the LDH sample traps more CO<sub>2</sub> and H<sub>2</sub>O at low RH, which may be associated with its textural properties (surface area, porosity, etc.). However, at 70% RH, weight gain proceeds faster on MgO than on the calcined LDH, and both samples gain in total ~12.5 wt %. Therefore, the calcined LDH sample seems to behave as MgO in the presence of CO<sub>2</sub> and H<sub>2</sub>O, favoring the production of hydrated MgCO<sub>3</sub>, or the magnesium hydroxyl-carbonate detected by XRD, instead of the LDH regeneration.

Finally, Figure 8 shows different isotherms performed on the calcined LDH sample, using RH and temperature as variables and the same CO<sub>2</sub> flow (100 mL/min). Isotherms performed with an RH of 40% behaved exponentially, and weight increased as a function of temperature, from 6.6 to 9.4 wt %. Then, if RH was increased to 50%, isotherms presented a different tendency. At 40 and 50 °C, samples gained weight as a function of temperature: 8.8 and 11.2 wt %, respectively. However, when temperature was increased to 60 and 70 °C, the weight gained decreased to 10.5 wt % in both cases. The results can be explained by water evaporation, accelerated when temperature was increased. Similar behaviors were observed in isotherms performed with RHs of 60 and 70%. Nevertheless, the final weight increments increased as a function of the RH. In fact, the largest weight increment was observed with a RH of 70% at 50 °C, being 16.4 wt %.

Comparing these results with others previously published,<sup>1,41</sup> it seems that CO<sub>2</sub> capture performed under these conditions is better. For example, da Costa and co-workers<sup>41</sup> captured CO<sub>2</sub> using water steam, but they performed experiments at 200 °C or higher temperatures. In that case, the weight increments observed varied between 2.7 and 4.8 wt %, which correspond to 0.61 and 1.08 mmol/g. Other papers have reported similar CO<sub>2</sub> absorption capacities of LDH samples.<sup>1,24,27,47</sup> Figure 9 shows

the thermogram performed at 1 °C/min, on the LDH sample humidity-treated at 50 °C and 70% RH, in order to complete all the different processes in the shortest temperature range. The thermogram produced a total weight lost of 17.1 wt % attributed to different dehydration, dehydroxylation, and decarbonation processes. The last weight decrement observed should correspond to the CO<sub>2</sub> desorbed, and it was equal to 9.5 wt %, which corresponds to 2.13 mmol/g. This result represents a better CO<sub>2</sub> capture on a LDH sample than those reported thus far. Additionally, in this case, the CO<sub>2</sub> capture was performed at a different temperature range (low temperatures).

## CONCLUSIONS

Dynamic H<sub>2</sub>O–CO<sub>2</sub> sorption experiments indicate that the native LDH sample did not present any kind of sorption process. On the other hand, the thermally calcined LDH sample registered significant weight increments during sorption experiments conducted under varying temperature and RH. Although the calcined sample did not regenerate the original layered structure (as in the N<sub>2</sub> flow<sup>35</sup>), TG, FTIR, and NMR results showed that weight increments corresponded to a double superficial process: hydration and carbonation. It seems that the superficial carbonation process occurred faster than hydroxylation, so the LDH regeneration was inhibited, favoring the MgCO<sub>3</sub> formation. The water adsorption was then produced on the superficial MgCO<sub>3</sub> previously formed. Although the LDH structure was not regenerated, the sample captured a considerable amount of CO<sub>2</sub>. Therefore, these results present a significant increment on the CO<sub>2</sub> absorption capacity (2.13 mmol/g) on this kind of material, in comparison to other papers previously published.

## AUTHOR INFORMATION

### Corresponding Author

\*Phone: +52 (55) 5622 4627. Fax: +52 (55) 5616 1371. E-mail: pfeiffer@iim.unam.mx.

## ACKNOWLEDGMENT

The authors thank M. A. Canseco-Martínez, G. Cedillo, and A. Tejeda for technical help, as well as financial support of the followings projects: PAPIIT-UNAM (IN100609) and ICyT-DF (179/2009).

## REFERENCES

- (1) Choi, S.; Drese, J. H.; Jones, C. W. Adsorbent materials for carbon dioxide capture from large anthropogenic point sources. *ChemSusChem* **2009**, *2*, 796–854.
- (2) Balat, H.; Oz, C. Applications of carbon dioxide capture and storage technologies in reducing emissions from fossil-fired power plants. *Energy Explor. Exploit.* **2007**, *25*, 357–362.
- (3) Orr, F. M., Jr. CO<sub>2</sub> capture and storage: Are we ready? *Energy Environ. Sci.* **2009**, *2*, 449–458.
- (4) Khatri, R. A.; Chuang, S. S. C.; Soong, Y.; Gray, M. Thermal and chemical stability of regenerable solid amine sorbent for CO<sub>2</sub> capture. *Energy Fuels* **2006**, *20*, 1514–1520.
- (5) Maceiras, R.; Alves, S. S.; Cancela, M. A.; Alvarez, E. Effect of bubble contamination on gas–liquid mass transfer coefficient on CO<sub>2</sub> absorption in amine solutions. *Chem. Eng. J.* **2008**, *137*, 422–427.
- (6) Chaffee, A. L.; Knowles, G. P.; Liang, Z. J.; Zhany, J.; Xiao, P.; Webley, P. A. CO<sub>2</sub> capture by adsorption: Materials and process development. *Inter. J. Greenhouse Gas Control* **2007**, *1*, 11–18.



- (7) Harlick, P. J. E.; Tezel, F. H. An experimental adsorbent screening study for CO<sub>2</sub> removal from N<sub>2</sub>. *Microporous Mesoporous Mater.* **2004**, *76*, 71–79.
- (8) Plant, D. F.; Maurin, G.; Deroche, I.; Llewellyn, P. Molecular dynamics simulation of the cation motion upon adsorption of CO<sub>2</sub> in faujasite zeolite systems. *J. Phys. Chem. B* **2006**, *110*, 14372–14378.
- (9) Diaz, E.; Muñoz, E.; Vega, A.; Ordoñez, S. Enhancement of the CO<sub>2</sub> retention capacity of γ-zeolites by Na and Cs treatments: Effect of adsorption temperature and water treatment. *Ind. Eng. Chem. Res.* **2008**, *47*, 412–418.
- (10) Siriwardane, R. V.; Shen, M. S.; Fisher, E. P.; Poston, J. A.; Shamsi, A. Adsorption of CO<sub>2</sub> on molecular sieves and activated carbon. *J. Energy Environ. Res.* **2009**, *1*, 19–27.
- (11) Hedin, N.; Chen, L. J.; Laaksonen, A. Sorbents for CO<sub>2</sub> capture from flue gas-aspects from materials and theoretical chemistry. *Nano-scale* **2010**, *2*, 1819–1841.
- (12) Chen, J.; Loo, L. S.; Wang, K. High pressure CO<sub>2</sub> adsorption on a polymer-derived carbon molecular sieve. *J. Chem. Eng. Data* **2008**, *53*, 2–4.
- (13) Kishimoto, Y.; Hata, K. Behaviors of single CO<sub>2</sub> molecule on pentagon at carbon nanotube tip observed by field emission microscopy. *Surf. Interface Anal.* **2008**, *40*, 1669–1672.
- (14) Pevida, C.; Plaza, M. G.; Arias, B.; Feroso, H.; Rubiera, F.; Pis, J. Surface modification of activated carbons for CO<sub>2</sub> capture. *Appl. Surf. Sci.* **2008**, *254*, 7165–7172.
- (15) Nair, B. N.; Burwood, R. P.; Goh, V. J.; Nakagawa, K.; Yamaguchi, T. Lithium based ceramic materials and membranes for high temperature CO<sub>2</sub> separation. *Prog. Mater. Sci.* **2009**, *54*, 511–541.
- (16) Alcérreca-Corte, I.; Fregoso-Israel, E.; Pfeiffer, H. CO<sub>2</sub> absorption on Na<sub>2</sub>ZrO<sub>3</sub>: A kinetic analysis of the chemisorption and diffusion processes. *J. Phys. Chem. C* **2008**, *112*, 6520–6525.
- (17) Mosqueda, H. A.; Vazquez, C.; Bosch, P.; Pfeiffer, H. Chemical sorption of carbon dioxide (CO<sub>2</sub>) on lithium oxide (Li<sub>2</sub>O). *Chem. Mater.* **2006**, *18*, 2307–2310.
- (18) Ávalos-Rendón, T.; Casa-Madrid, J.; Pfeiffer, H. Thermochemical capture of carbon dioxide on lithium aluminates (LiAlO<sub>2</sub> and Li<sub>5</sub>AlO<sub>4</sub>): A new option for the CO<sub>2</sub> absorption. *J. Phys. Chem. A* **2009**, *113*, 6919–6923.
- (19) Lu, D. Y.; Hughes, R. W.; Anthony, E. J.; Manovic, V. Sintering and reactivity of CaCO<sub>3</sub>-based sorbents for in situ CO<sub>2</sub> capture in fluidized beds under realistic calcination conditions. *J. Environ. Eng.* **2009**, *135*, 404–410.
- (20) Manovic, V.; Anthony, E. CaO-based pellets supported by calcium aluminate cements for high-temperature CO<sub>2</sub> capture. *Environ. Sci. Technol.* **2009**, *43*, 7117–7122.
- (21) Martavaltzi, C. S.; Lemonidou, A. A. Development of new CaO based sorbent materials for CO<sub>2</sub> removal at high temperature. *Microporous Mesoporous Mater.* **2008**, *110*, 119–127.
- (22) Lee, S. C.; Chae, H. J.; Lee, S. J.; Choi, B. Y.; Yi, C. K.; Ryu, C. K.; Kim, J. C. Development of regenerable MgO-based sorbent promoted with K<sub>2</sub>CO<sub>3</sub> for CO<sub>2</sub> capture at low temperatures. *Environ. Sci. Technol.* **2008**, *42*, 2736–2741.
- (23) Philipp, R.; Fujimoto, K. FTIR spectroscopic study of carbon dioxide adsorption/desorption on magnesia/calcium oxide catalysts. *J. Phys. Chem.* **1992**, *96*, 9035–9038.
- (24) Ding, Y.; Alpay, E. Equilibria and kinetics of CO<sub>2</sub> adsorption on hydrotalcite adsorbent. *Chem. Eng. Sci.* **2000**, *55*, 3461–3474.
- (25) Oliveira, E. L. G.; Grande, C. A.; Rodrigues, A. E. CO<sub>2</sub> sorption on hydrotalcite and alkali-modified (K and Cs) hydrotalcites at high temperatures. *Sep. Purif. Tech.* **2008**, *62*, 137–147.
- (26) Yong, Z.; Rodrigues, A. E. Hydrotalcite-like compounds as adsorbents for carbon dioxide. *Energy Convers. Manag.* **2002**, *43*, 1865–1876.
- (27) Reijers, H. T. J.; Valster-Schiermeier, S. E. A.; Cobden, P. D.; van der Brink, R. W. Hydrotalcite as CO<sub>2</sub> sorbent for sorption-enhanced steam reforming of methane. *Ind. Eng. Chem. Res.* **2006**, *45*, 2522–2530.
- (28) Cavani, F.; Trifiro, F.; Vaccari, A. Hydrotalcite-type anionic clays: Preparation, properties and applications. *Catal. Today* **1991**, *11*, 173–301.
- (29) Rives, V. *Layered Double Hydroxides: Present and Future*; Nova Science Publishers: New York, 2001.
- (30) Duan, X.; Evans, D. G., Eds. In *Layered Double Hydroxides*; Springer-Verlag: Berlin-Heidelberg, Germany, 2006.
- (31) Figueras, F. Base catalysis in the synthesis of fine chemicals. *Top. Catal.* **2004**, *29*, 189–196.
- (32) Sels, B. F.; De Vos, D. E.; Jacobs, P. A. Hydrotalcite-like anionic clays in catalytic organic reactions. *Catal. Rev.* **2001**, *43*, 443–488.
- (33) Rao, K. K.; Gravelle, M.; Valente, J. S.; Figueras, F. Activation of Mg–Al hydrotalcite catalysts for aldol condensation reactions. *J. Catal.* **1998**, *173*, 115–121.
- (34) Kumbhar, P. S.; Valente, J. S.; Millet, J. M.; Figueras, F. Mg–Fe hydrotalcite as a catalyst for the reduction of aromatic nitro compounds with hydrazine hydrate. *J. Catal.* **2000**, *191*, 467–473.
- (35) Cantú, M.; López-Salinas, E.; Valente, J. S.; Montiel, R. SO<sub>x</sub> removal by calcined MgAlFe hydrotalcite-like materials: Effect of the chemical composition and the cerium incorporation method. *Environ. Sci. Technol.* **2005**, *39*, 9715–9720.
- (36) Sanchez-Cantu, M.; Perez-Diaz, L. M.; Maubert, A. M.; Valente, J. S. Dependence of chemical composition of calcined hydrotalcite-like compounds for SO<sub>x</sub> reduction. *Catal. Today* **2010**, *150*, 332–339.
- (37) Pfeiffer, H.; Lima, E.; Lara, V.; Valente, J. S. Thermokinetic study of the rehydration process of a calcined MgAl-layered double hydroxide. *Langmuir* **2010**, *26*, 4074–4079.
- (38) Wang, X. P.; Yu, J. J.; Cheng, J.; Hao, Z. P.; Xu, Z. P. High-temperature adsorption of carbon dioxide on mixed oxides derived from hydrotalcite-like compounds. *Environ. Sci. Technol.* **2008**, *42*, 614–618.
- (39) Lwin, Y.; Abdullah, F. High temperature adsorption of carbon dioxide on Cu–Al hydrotalcite-derived mixed oxides: kinetics and equilibria by thermogravimetry. *J. Therm. Anal. Calorim.* **2009**, *97*, 885–889.
- (40) Reddy, M. K. R.; Xu, Z. P.; Lu, G. Q.; da-Costa, J. C. D. Effect of SO<sub>x</sub> adsorption on layered double hydroxides for CO<sub>2</sub> capture. *Ind. Eng. Chem. Res.* **2008**, *47*, 7357–7360.
- (41) Reddy, M. K. R.; Xu, Z. P.; Lu, G. Q.; da-Costa, J. C. D. Influence of water on high-temperature CO<sub>2</sub> capture using layered double hydroxide derivatives. *Ind. Eng. Chem. Res.* **2008**, *47*, 2630–2635.
- (42) Meis, N. N. A. H.; Bitter, J. H.; de Jong, K. P. On the influence and role of alkali metals on supported and unsupported activated hydrotalcites for CO<sub>2</sub> sorption. *Ind. Eng. Chem. Res.* **2010**, *49*, 8086–8093.
- (43) Meis, N. N. A. H.; Bitter, J. H.; de Jong, K. P. Support and size effects of activated hydrotalcites for precombustion CO<sub>2</sub> capture. *Ind. Eng. Chem. Res.* **2010**, *49*, 1229–1235.
- (44) Yavuz, C. T.; Shinall, B. D.; Iretskii, A. V.; White, M. G.; Golden, T.; Atihan, M.; Ford, P. C.; Stucky, G. D. Markedly improved CO<sub>2</sub> capture efficiency and stability on gallium substituted hydrotalcites at elevated temperatures. *Chem. Mater.* **2009**, *21*, 3473–3475.
- (45) Reynolds, S. P.; Ebner, A. D.; Ritter, J. A. Carbon dioxide capture from flue gas by pressure swing adsorption at high temperature using a K-promoted HTlc: Effects of mass transfer on the process performance. *Environ. Prog.* **2006**, *25*, 334–342.
- (46) Reynolds, S. P.; Ebner, A. D.; Ritter, J. A. Stripping PSA cycles for CO<sub>2</sub> recovery from flue gas at high temperature using a hydrotalcite-like adsorbent. *Ind. Eng. Chem. Res.* **2006**, *45*, 4278–4294.
- (47) Ebner, A. D.; Reynolds, S. P.; Ritter, J. A. Nonequilibrium kinetic model that describes the reversible adsorption and desorption behavior of CO<sub>2</sub> in a K-promoted hydrotalcite-like compound. *Ind. Eng. Chem. Res.* **2007**, *46*, 1737–1744.
- (48) Yong, Z.; Mata, V.; Rodrigues, A. E. Adsorption of carbon dioxide onto hydrotalcite-like compounds (HTlcs) at high temperatures. *Ind. Eng. Chem. Res.* **2001**, *40*, 204–209.
- (49) Hufton, J. R.; Mayorga, S.; Sincara, S. Sorption-enhanced reaction process for hydrogen production. *AIChE J.* **1999**, *45*, 248–256.
- (50) Pfeiffer, H.; Martínez-dlCruz, L.; Lima, E.; Flores, J.; Valente, J. S. Influence of Mg/Al ratio on the thermokinetic rehydration of calcined Mg–Al layered double hydroxides. *J. Phys. Chem. C* **2010**, *114*, 8485–8492.



(51) Lowell, S.; Shiels, J. E.; Thomas, M. A.; Thommes, M. *Characterization of Porous Solids and Powders: Surface Area, Pore Size, and Density*; Kluwer Academic Publishers: Dordrecht, The Netherlands, 2004.

(52) Levenspiel, O. *Chemical Reaction Engineering*; John Wiley & Sons: New York, 1999.

(53) Rodríguez-Mosqueda, R.; Pfeiffer, H. Thermokinetic analysis of the CO<sub>2</sub> chemisorption on Li<sub>4</sub>SiO<sub>4</sub> by using different gas flow rates and particle sizes. *J. Phys. Chem. A* **2010**, *114*, 4535–4541.

(54) Hibino, T.; Tsunashima, A. Characterization of repeatedly reconstructed Mg-Al hydrotalcite-like compounds: Gradual segregation of aluminum from the structure. *Chem. Mater.* **1998**, *10*, 4055–4061.

(55) Martínez-Ortiz, M. J.; Lima, E.; Lara, V.; Méndez-Vivar, J. Structural and textural evolution during folding of layers of layered double hydroxides. *Langmuir* **2008**, *24*, 8904–8911.

(56) Lippmaa, E.; Samoson, A.; Magi, M. High resolution <sup>27</sup>Al NMR of aluminosilicates. *J. Am. Chem. Soc.* **1986**, *108*, 1730–1735.

(57) Martínez-Gallegos, S.; Pfeiffer, H.; Lima, E.; Espinosa, M.; Bosch, P.; Bulbulian, S. Cr(VI) immobilization in mixed (Mg, Al) oxides. *Microporous Mesoporous Mater.* **2006**, *94*, 234–242.